Laser-pulse compression using magnetized plasmas

Yuan Shi,[1,2,*] Hong Qin,[1,2,3] and Nathaniel J. Fisch[1,2]

[1]*Department of Astrophysical Sciences, Princeton University, Princeton, New Jersey 08544, USA*

[2]*Princeton Plasma Physics Laboratory, Princeton University, Princeton, New Jersey 08543, USA*

[3]*School of Nuclear Science and Technology, University of Science and Technology of China, Hefei, Anhui 230026, China*

(Received 2 September 2016; revised manuscript received 29 December 2016; published 28 February 2017)

Proposals to reach the next generation of laser intensities through Raman or Brillouin backscattering have centered on optical frequencies. Higher frequencies are beyond the range of such methods mainly due to the wave damping that accompanies the higher-density plasmas necessary for compressing higher frequency lasers. However, we find that an external magnetic field transverse to the direction of laser propagation can reduce the required plasma density. Using parametric interactions in magnetized plasmas to mediate pulse compression, both reduces the wave damping and alleviates instabilities, thereby enabling higher frequency or lower intensity pumps to produce pulses at higher intensities and longer durations. In addition to these theoretical advantages, our method in which strong uniform magnetic fields lessen the need for high-density uniform plasmas also lessens key engineering challenges or at least exchanges them for different challenges.

DOI: 10.1103/PhysRevE.95.023211

Extremely high intensity lasers could have manifold applications, such as inertial confinement fusion [1] and single molecule imaging [2]. To achieve extreme intensities, parametric compressions have been proposed using plasmas with waves, such as the Langmuir wave and the ion acoustic wave mediating the compression [3–5]. At optical frequencies, a window exists in the plasma density-temperature space wherein neither the plasma waves nor the lasers are heavily damped. However, for higher frequency lasers, higher-density plasmas are required to mediate the interaction, and at higher densities these waves tend to be heavily damped. Here we propose, by utilizing waves in magnetized plasmas, to extend the frequency and intensity range of laser pulse compression. In magnetized plasmas, waves that can be utilized are the electrostatic waves, including hybrid waves and Bernstein waves. These waves provide resonances in which contributions from plasma density are partially replaced by more controllable contributions from the external magnetic field. The reduced dependence on plasma density alleviates wave damping as well as deleterious instabilities [6], expanding the operation window of pulse compression to produce output pulses at both higher intensities and longer durations.

In this paper, we show the advantage of applying a transverse magnetic field by examining pulse compression mediated by the upper-hybrid (*UH*) wave. The transverse geometry differs from recent considerations of axial magnetic fields, which affect other aspects of propagation and amplification [7]. Consider the case where the lasers propagate exactly perpendicular to the external magnetic field, which lends itself naturally to the main application where the amplified pulse is focused onto a distant target (Fig. 1). For propagation perpendicular to the magnetic field, the linear wave eigenmodes are well known [8]. One electromagnetic eigenmode is the *O* wave with the wave electric field parallel to the external magnetic field, obeying the dispersion relation $n_\perp^2 = 1 - \omega_p^2/\omega^2$. Here $n_\perp = ck_\perp/\omega$ is the refractive index, and ω_p is the plasma frequency. The other electromagnetic eigenmode is the *X* wave, which hybridizes with the electrostatic eigenmode, the *UH* wave, obeying the dispersion relation $n_\perp^2 = 2RL/(R+L)$. Here $R, L = 1 - \omega_p^2/[\omega(\omega \pm \Omega)]$, where $\Omega = eB_0/m_e$ is the electron gyrofrequency. The electric field of both the *X* wave and the *UH* wave are in the plane perpendicular to the magnetic field. Although an *X* wave and an *O* wave couple only weakly, two *X* waves or two *O* waves couple strongly through the *UH* wave.

What we show here is that compression of these electromagnetic waves mediated by the *UH* wave is described by the same equations that describe mediation by the Langmuir wave, except for the coupling coefficient. However, because less density is sufficient to accomplish the resonance, key deleterious effects become less competitive. The result is an expansion of the parameter regime of operation, allowing extension even to the x-ray regime whenever fields of several hundred megagauss to a gigagauss become available. Although such fields are challenging, at the cusp of present feasibility, our new method at least provides a theoretical opportunity to compress lasers that otherwise could not be compressed. In addition, at lower frequencies, more readily available magnetic fields may also confer advantages.

To see this, consider the resonant coupling between the pump laser (with frequency ω_1) and the seed pulse (with frequency ω_2) through the mediating *UH* wave (with frequency $\omega_3 = \sqrt{\omega_p^2 + \Omega^2}$). This interaction can be described by the three-wave equations [9]. Using the three-wave resonance conditions, it can be shown that in the limit $\omega_0 := \omega_1 \simeq \omega_2 \gg \omega_3$, both electromagnetic eigenmodes are transverse with little dispersion and the *UH* wave is almost longitudinal with approximately zero group velocity. Consequently, the three-wave interaction in the magnetized case has one-to-one correspondence with that in the cold unmagnetized case,

$$\begin{aligned}(\partial_t + c\partial_x)a_1 &= \frac{\omega_p}{2}a_2 a_3,\\ (\partial_t - c\partial_x)a_2 &= -\frac{\omega_p}{2}a_1 a_3^*,\\ \partial_t a_3 &= -\frac{\omega_0\omega_p}{2\omega_3}a_1 a_2^*.\end{aligned} \tag{1}$$

*yshi@pppl.gov

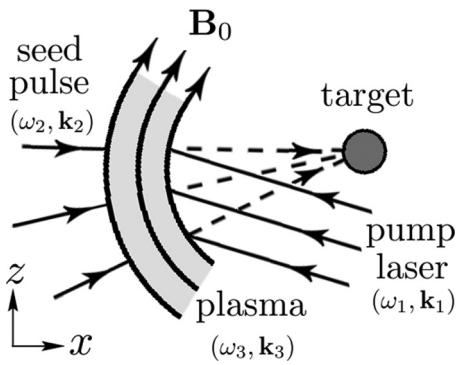

FIG. 1. Amplifying and focusing a seed pulse by stimulated backscattering of a pump laser in magnetized plasma.

The electric field amplitude of the pump and the seed are normalized by $a_{1,2} = eE_{1,2}/m_e c\omega_{1,2}$, and the amplitude of the *UH* wave is normalized by $a_3 = eE_3/m_e c\omega_p$. The linear growth rate, i.e., for negligible pump depletion, is

$$\Gamma_R = \frac{\sqrt{\omega_3\omega_0}}{2}|a_1|\gamma_B^{-1}, \tag{2}$$

where $\gamma_B := \omega_3/\omega_p > 1$ measures the extent to which plasma density is replaced by a magnetic field in the *UH* resonance. Except for the above modification, the solution in the nonlinear stage is the same as the unmagnetized cases. However, the physical processes that limit pulse compression are different. What is of critical importance is that these physical processes lead to different constraints on the possible amplification regimes.

The first limiting effect is wave breaking, which limits the maximum pump intensity that can be used for amplifying the pulse. In magnetized plasmas, the wave breaking intensity is modified by the Lorentz force, and the *UH* wave breaks when the electron quiver velocity in the $\mathbf{k}_3$ direction $v_q \simeq eE_3\omega_3/m_e\omega_p^2$ exceeds the wave phase velocity $v_p = \omega_3/k_3 \simeq c\omega_3/2\omega_0$ [10]. The condition $v_q \lesssim v_p$, which guarantees that the *UH* wave remains unbroken, can be rewritten in terms of a constraint on the pump intensity $I_1 = 8I_c|a_1|^2$ using the Manley-Rowe relation, which constrains the maximum amplitude of the *UH* wave to be $|a_3| \leqslant \sqrt{\omega_0/\omega_3}|a_1|$. The resultant sufficient condition that the *UH* wave remains unbroken is

$$I_1 \lesssim I_c\left(\frac{\omega_3}{\omega_0}\right)^3\gamma_B^{-2}, \tag{3}$$

where $I_c = n_c m_e c^3/16$ and $n_c = \epsilon_0 m_e\omega_0^2/e^2$ is the critical density. When more plasma density is replaced by a magnetic field in ω_3, less energy can be contained in the *UH* wave, giving rise to the γ_B^{-2} reduction. For given laser parameters, wave breaking constrains the minimum plasma density as well as the maximum magnetic field.

The second limiting effect is the modulational instability with growth rate [3,6],

$$\Gamma_M = \frac{\omega_3^2}{8\omega_0}|a|^2\gamma_B^{-2}. \tag{4}$$

The maximum time that the pulse can be amplified by the pump is limited to a few inverse growth rates. Since $\Gamma_M \ll \Gamma_R$ even at the wave breaking intensity, this instability does not prevent the amplification from reaching the nonlinear stage, which can continue until

$$t_M \approx \left(12\,\delta\Lambda_0^2\right)^{1/3}\frac{\gamma_B^{4/3}}{\omega_3 a_{10}^{4/3}}, \tag{5}$$

where $\delta = \int\Gamma_M dt \sim 1$ is the accumulated phase shift, Λ_0 is the number of linear exponentiations before the nonlinear stage is reached, and a_{10} is the initial pump amplitude. The largest pulse compression is attained at the maximum compression time t_M, which gives the highest leading spike intensity $I_2 \approx 16I_c(3\delta/\Lambda_0)^{2/3}(2a_{10})^{4/3}\gamma_B^{2/3}\omega_0/\omega_3$ and the shortest spike duration $\Delta t_2 \approx 2(2\Lambda_0/3\delta)^{1/3}a_{10}^{-2/3}\gamma_B^{2/3}/\omega_0$. Ramping up the pump intensity while keeping plasma parameters fixed, the maximum output intensity is reached using the most intense pump allowed by wave breaking, which gives $I_2 \leqslant 16I_c(3\delta/2\Lambda_0)^{2/3}\gamma_B^{-2/3}\omega_3/\omega_0$. Alternatively, optimizing plasma parameters while keeping lasers fixed, the maximum output intensity is reached using the smallest possible ω_3 allowed by wave breaking, which gives $I_2 \leqslant 8I_c(3\delta a_{10}/2\Lambda_0)^{2/3}$, independent of γ_B. Note that this output intensity could have been achieved using unmagnetized plasmas if wave breaking and longitudinal modulational instability were the only limiting effects.

The third limiting effect is the collisionless damping of the *UH* wave. Although linear collisionless damping vanishes when the wave propagates exactly perpendicular to the magnetic field [8,11], nonlinear collisionless damping persists due to surfatron acceleration [12] and stochastic heating [13]. To give a conservative estimation, note that the *UH* frequency is typically comparable to the gyrofrequency. Hence an electron having perpendicular velocity close to v_p sees an almost constant wave electric field. In such an electric field, the electron may gain or lose energy from the wave, depending on the relative phase of wave motion and gyromotion. The phase mixing process causes the *UH* wave to damp on a Maxwellian background with rate $\nu_L \approx \sqrt{\pi}(v_p/v_T)^3\exp(-v_p^2/v_T^2)\omega_p^2/\omega_3$, where v_T is the thermal velocity. Since a weakly damped linear wave requires $v_p > v_T$, the sufficient condition that collisionless damping is weak may be approximated as

$$\frac{\nu_L}{\omega_3} \approx \sqrt{\pi}(3/2)^{3/2}e^{-v_p^2/v_T^2}\gamma_B^{-2} \ll 1. \tag{6}$$

As $\omega_3 \to |\Omega|$, the electron density vanishes, so there are fewer electrons to participate in phase mixing, and collisionless damping consequently diminishes.

The fourth limiting effect is collisional damping of both the lasers and the *UH* wave, whose rates decrease rapidly when plasma density decreases. Collisional damping arises since the electron quiver motion is randomized by electron-ion collisions, thermalizing the wave energy carried by electrons. The collisional damping rate of the *UH* wave and lasers are $\nu_3 \approx \nu_{ei}(1 - \omega_p^2/2\omega_3^2)$ and $\nu_0 \approx \nu_{ei}\omega_p^2/2\omega_0^2$, respectively. The collision frequency $\nu_{ei} \approx n_e Z^2 e^4\Lambda/(4\pi\epsilon_0)^2 m_e^2 v^3$, where Z is the ion charge, Λ is the Coulomb logarithm, and v is the characteristic velocity of electrons, containing contributions from both thermal motion and wave motion. Ignoring wave motion, an upper bound of the collision frequency can be obtained. This upper bound gives sufficient conditions that

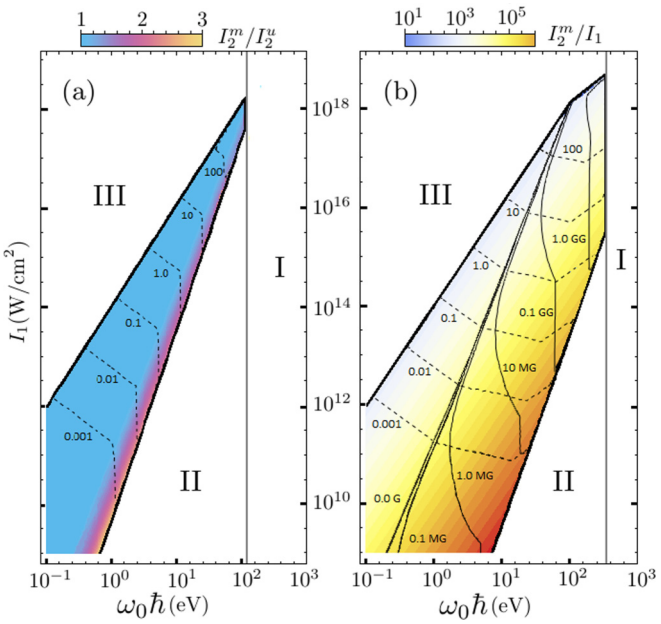

FIG. 2. Operation windows in the pump laser parameter space (colored regions). Regions I–III are excluded by limiting effects and fluid model constraints. (a) The operation window when $B_0 = 0$. The color scale compares the maximum output achievable in the magnetized case I_2^m versus that in the unmagnetized case I_2^u. The dashed contours (in units of 10^{20} cm^{-3}) are plasma density necessary for achieving I_2^u. (b) The expanded operation window when $B_0 \geqslant 0$. The color scale is the gain I_2^m/I_1. By applying minimal magnetic fields (solid contours), plasma densities (dashed contours) necessary for achieving I_2^m are reduced.

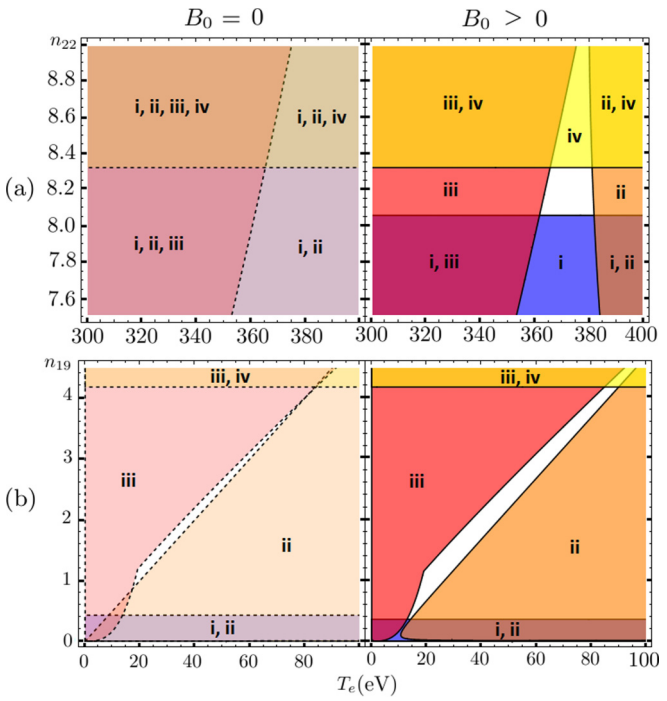

FIG. 3. Operation windows in the plasma parameter space (white regions). The colored regions, possibly overlapping, are excluded by wave breaking [blue (i)], collisionless [orange (ii)] or collisional damping [red (iii)], and $\omega_3/\omega_0 > 0.1$ [yellow (iv)]. The exclusions in unmagnetized plasmas (left) are larger than those in magnetized plasmas (right). (a) Soft x-ray laser with $I_1 = 10^{18}$ W/cm^2 and $\omega_0\hbar = 250$ eV. $B_0 = 1.5$ GG. (b) KrF laser with $I_1 = 10^{13}$ W/cm^2 and $\omega_0\hbar = 5$ eV. $B_0 = 5$ MG. n_{19} and n_{22} are n_e in the units of 10^{19} and 10^{22} cm^{-3}.

collisional damping is weak,

$$\nu_3 \Delta t_2 \lesssim 1, \quad \nu_0 t_M/2 \lesssim 1. \tag{7}$$

The first condition ensures that the *UH* wave remains weakly damped during the seed transient time. The second condition ensures that the lasers can penetrate the plasma with little energy loss. These two conditions combined are stricter than $\nu_0\nu_3 < \Gamma_R^2$, the condition that the parametric instability can be excited provided that $\Lambda_0 \geqslant 2$. By replacing n_e with B_0 in ω_3, the collisional damping constraints on the *UH* wave and the lasers are alleviated by $\gamma_B^{-4/3}$ and $\gamma_B^{-8/3}$, respectively, when pulse compression uses the maximum time t_M. When less time is used, the pulse duration becomes longer, so the constraints become stricter for the *UH* wave whereas less strict for the lasers. For given laser frequencies, the reduction of wave damping results in higher pulse compression efficiency.

These four limiting effects define an operation window within which efficient pulse compression is theoretically possible. By adjusting the extra parameter γ_B, the unmagnetized operation window can be expanded. First, consider expansion of the operation window in ω_0-I_1 space. For example, consider pulse compression in hydrogen plasmas (Fig. 2), and replace conditions of the type $x \ll y$ by $x/y < 0.1$. The unmagnetized operation window (a) can be maximally expanded to (b) when external magnetic fields (black contours) are applied. In these figures, region I is excluded because collisionless damping becomes strong while keeping the plasma condition $n_e\lambda_D^3 \gg 1$; region II is excluded, because both damping mechanisms are strong; region III is excluded because the wave breaking limit is exceeded while keeping $\omega_3 \ll \omega_0$. Second, note the increase in the maximum achievable output intensity from I_2^u in the unmagnetized case to I_2^m in the magnetized case. This improvement is enabled by the alleviation of the modulational instability and wave damping because the requisite plasma density (dashed contours) is now smaller.

To illustrate the expanded regime made possible through magnetizing plasmas, consider the very ambitious and speculative compression of soft x-ray pulses. For example, x-ray pulses produced at the Linac Coherent Light Source have 2–6 mJ in energy, 5–500 fs in duration, and focal spots of $\sim$10 μm^2 [14], corresponding to intensities of $\sim 10^{18}$ W/cm^2. Since the photon energy in these pulses is in the range of 250 eV–10 KeV, efficient pulse compression using unmagnetized plasmas is not possible (Fig. 2). However, the inefficient compression using unmagnetized plasmas [15] can be made efficient by applying a magnetic field on the order of gigagauss [Fig. 3(a)] using hydrogen plasmas. Such a field is of course huge but, in principle, achievable over the small volumes; for compressing a 500-fs pulse, a plasma length of only 0.3 mm is needed. The strong magnetic field reduces necessary plasma density and therefore reduces wave damping, making it theoretically possible to compress picosecond x-ray pulses

TABLE I. Key parameters for examples given in Fig. 3, assuming the initial pulse duration is not much longer than Δt_2, and the initial pulse intensity is such that $\Lambda_0 \approx 6$. For soft x-ray pulses, applying a magnetic field opens up the otherwise closed operation window. For KrF pulses, applying a magnetic field reduces the necessary plasma density and enables more intense and longer outputs.

Pump	Plasma		Pulse		Compression		
	B_0	min n_e	max I_2/I_1	Δt_2	γ_B	t_M	ω_3/ω_0 (%)
250 eV, I_{18}	1.5 GG	$8.1n_{22}$	2.3×10^3	0.5 fs	1.9	0.9 ps	8.1
5 eV, I_{13}	0 G	$8.9n_{18}$	1.9×10^4	54 fs	1.0	0.8 ns	2.2
	5 MG	$3.6n_{18}$	2.7×10^4	65 fs	1.3	1.3 ns	1.8

to femtoseconds (Table I). In this example, the magnetic field opens up the otherwise closed operation window.

To illustrate the use of magnetized plasma in a more practicable example, consider the compression of KrF pulses. For example, KrF pulses produced at the Nike Laser Facility have kilojoules energy with nanosecond durations [16]. These pulses can be focused on a spot of sizes ~ 0.01 cm^2, reaching peak intensities of $\sim 10^{14}$ W/cm^2. The average intensity, however, falls in the range of 10^{12}–10^{13} W/cm^2. Since the photon energy of the KrF laser is ~ 5 eV, the unmagnetized operation window is about to close when the laser intensity is at the lower end (Fig. 2). However, the narrow unmagnetized window can be expanded by applying a megagauss magnetic field [Fig. 3(b)], when hydrocarbon plasmas (C_3H_8, $Z_{\text{eff}} \approx 2.36$) are used. In the expanded operation window, the minimum plasma density is reduced, which enables the output pulse to have larger intensities and longer durations (Table I). In this example, less density is required, and more intense output can be produced using magnetized plasma.

Apart from the direct benefit of an expanded operating window, note that replacing plasma density by a magnetic field is advantageous because the magnetic field uniformity is much more controllable. This technological advantage makes it beneficial to use magnetized plasma within the region where $I_2^m = I_2^u$ (Fig. 2), even when it does not improve the maximum output intensity.

To achieve resonant parametric pulse compression in experiments, it is necessary to produce plasma targets not only with specific densities and temperatures, but also with sufficient uniformity. Unmagnetized targets satisfying these requirements are in principle attainable but in practice challenging. The laboratory standard is to ionize a gas jet [17]. This is appropriate for plasma targets with densities less than 10^{20} cm^{-3}, temperatures of $\sim 10^1$ eV, and sizes of ~ 1 mm. Producing unmagnetized targets of higher densities has been envisioned using a dense aerosol jet [18]. However, reaching high temperature and uniformity with these targets has not been demonstrated experimentally.

The technological challenge in making high-density uniform plasmas is reduced if we compress pulses using magnetized plasmas instead, in which the requisite density is smaller. Moreover, the constancy of ω_3 depends less on the uniformity of plasma density, which is usually harder to control compared to external magnetic fields. One technique generates strong magnetic field by driving capacitor-coil targets with intense lasers. In a number of experiments [19], generation of megagauss magnetic fields, which is uniform on the millimeter scale and quasistatic on the nanosecond scale, has been demonstrated. Another technique generates strong magnetic field by ablating solid targets with intense laser pulses [20–22]. This technique can produce plasmas with $\sim 10^{21}$ cm^{-3} densities and magnetic fields on the order of gigagauss when picosecond pulses with ~ 1 μm wavelengths and $\sim 10^{20}$ W/cm^2 intensities are used in experiments. The densities and magnetic fields produced near the solid surfaces are uniform on the micrometer scale and quasistatic on the picosecond scale. The usefulness of strong magnetic fields justifies further development of these technologies.

To summarize, our method enables compression of powerful lasers beyond the reach of currently envisioned methods. By substituting the requirement for high plasma density with one for an external magnetic field, the mediating wave is then the upper-hybrid wave rather than the Langmuir wave. Deleterious physical effects associated with high plasma density are alleviated, and the engineering requirements of producing high and uniform plasma densities can be relaxed. Thus, using magnetized plasmas, we can significantly expand the operation window and achieve efficient pulse compression for higher frequencies and lower intensity pumps, producing pulses of both higher intensities and longer durations.

The work was supported by NNSA Grant No. DE-NA0002948, AFOSR Grant No. FA9550-15-1-0391, and DOE Research Grant No. DEAC02-09CH11466.

[1] R. L. Kauffman, L. J. Suter, C. B. Darrow, J. D. Kilkenny, H. N. Kornblum, D. S. Montgomery, D. W. Phillion, M. D. Rosen, A. R. Theissen, R. J. Wallace, and F. Ze, Phys. Rev. Lett. **73**, 2320 (1994).

[2] J. C. Solem and G. C. Baldwin, Science **218**, 229 (1982); R. Neutze, R. Wouts, D. van der Spoel, E. Weckert, and J. Hajdu, Nature (London) **406**, 752 (2000); S. P. Hau-Riege, R. A. London, H. N. Chapman, A. Szoke, and N. Timneanu, Phys. Rev. Lett. **98**, 198302 (2007).

[3] R. D. Milroy, C. E. Capjack, and C. R. James, Phys. Fluids **22**, 1922 (1979); C. E. Capjack, C. R. James, and J. N. McMullin, J. Appl. Phys. **53**, 4046 (1982); V. M. Malkin, G. Shvets, and N. J. Fisch, Phys. Rev. Lett. **82**, 4448 (1999).

[4] A. A. Andreev, C. Riconda, V. T. Tikhonchuk, and S. Weber, Phys. Plasmas **13**, 053110 (2006); S. Weber, C. Riconda, L. Lancia, J.-R. Marquès, G. A. Mourou, and J. Fuchs, Phys. Rev. Lett. **111**, 055004 (2013); A. Frank, J. Fuchs, L. Lancia, G. Lehmann, J.-R. Marquès, G. Mourou, C. Riconda, K. Spatschek, T. Toncian, L. Vassura, and S. Weber, Eur. Phys. J: Spec. Top. **223**, 1153 (2014); G. Lehmann and K. H. Spatschek, Phys. Plasmas **23**, 023107 (2016).

[5] C. Riconda, S. Weber, L. Lancia, J.-R. Marqus, G. A. Mourou, and J. Fuchs, Phys. Plasmas **20**, 083115 (2013); Q. Jia, I. Barth, M. R. Edwards, J. M. Mikhailova, and N. J. Fisch, *ibid.* **23**, 053118 (2016).

[6] D. S. Clark and N. J. Fisch, Phys. Plasmas **10**, 3363 (2003); V. M. Malkin, N. J. Fisch, and J. S. Wurtele, Phys. Rev. E **75**, 026404 (2007); V. M. Malkin and N. J. Fisch, Eur. Phys. J: Spec. Top. **223**, 1157 (2014).

[7] S. Vij, T. S. Gill, and M. Aggarwal, Phys. Plasmas **23**, 123111 (2016); M. Shoucri, Laser Part. Beams **34**, 315 (2016); S. X. Luan, W. Yu, F. Y. Li, D. Wu, Z. M. Sheng, M. Y. Yu, and J. Zhang, Phys. Rev. E **94**, 053207 (2016).

[8] T. Stix, *Waves in Plasmas* (Springer, New York, 1992).

[9] T. Boyd and J. Turner, J. Math. Phys. **19**, 1403 (1978); C. Grebogi and C. Liu, Phys. Fluids **23**, 1330 (1980).

[10] M. Karmakar, C. Maity, and N. Chakrabarti, Phys. Plasmas **23**, 064503 (2016).

[11] A. I. Sukhorukov and P. Stubbe, Phys. Plasmas **4**, 2497 (1997).

[12] R. Z. Sagdeev and V. D. Shapiro, ZhETF Pis. Red. **17**, 389 (1973) [JETP Lett. **17**, 279 (1973)]; J. M. Dawson, V. K. Decyk, R. W. Huff, I. Jechart, T. Katsouleas, J. N. Leboeuf, B. Lembege, R. M. Martinez, Y. Ohsawa, and S. T. Ratliff, Phys. Rev. Lett. **50**, 1455 (1983).

[13] C. F. F. Karney, Phys. Fluids **21**, 1584 (1978); **22**, 2188 (1979).

[14] C. Bostedt, J. D. Bozek, P. H. Bucksbaum, R. N. Coffee, J. B. Hastings, Z. Huang, R. W. Lee, S. Schorb, J. N. Corlett, P. Denes, P. Emma, R. W. Falcone, R. W. Schoenlein, G. Doumy, E. P. Kanter, B. Kraessig, S. Southworth, L. Young, L. Fang, M. Hoener, N. Berrah, C. Roedig, and L. F. DiMauro, J. Phys. B: At., Mol. Opt. Phys. **46**, 164003 (2013).

[15] J. D. Sadler, R. Nathvani, P. Olekiewicz, L. A. Ceurvorst, N. Ratan, M. F. Kasim, R. M. G. M. Trines, R. Bingham, and P. A. Norreys, Sci. Rep. **5**, 16755 (2015).

[16] S. P. Obenschain, S. E. Bodner, D. Colombant, K. Gerber, R. H. Lehmberg, E. A. McLean, A. N. Mostovych, M. S. Pronko, C. J. Pawley, A. J. Schmitt, J. D. Sethian, V. Serlin, J. A. Stamper, C. A. Sullivan, J. P. Dahlburg, J. H. Gardner, Y. Chan, A. V. Deniz, J. Hardgrove, T. Lehecka, and M. Klapisch, Phys. Plasmas **3**, 2098 (1996).

[17] Y. Ping, W. Cheng, S. Suckewer, D. S. Clark, and N. J. Fisch, Phys. Rev. Lett. **92**, 175007 (2004); W. Cheng, Y. Avitzour, Y. Ping, S. Suckewer, N. J. Fisch, M. S. Hur, and J. S. Wurtele, *ibid.* **94**, 045003 (2005); L. Lancia, J.-R. Marquès, M. Nakatsutsumi, C. Riconda, S. Weber, S. Hüller, A. Mančić, P. Antici, V. T. Tikhonchuk, A. Héron, P. Audebert, and J. Fuchs, *ibid.* **104**, 025001 (2010); L. Lancia, A. Giribono, L. Vassura, M. Chiaramello, C. Riconda, S. Weber, A. Castan, A. Chatelain, A. Frank, T. Gangolf, M. N. Quinn, J. Fuchs, and J.-R. Marquès, *ibid.* **116**, 075001 (2016).

[18] M. J. Hay, E. J. Valeo, and N. J. Fisch, Phys. Rev. Lett. **111**, 188301 (2013); D. Ruiz *et al.*, J. Aerosol Sci. **76**, 115 (2014).

[19] S. Fujioka *et al.*, Sci. Rep. **3**, 1170 (2013); J. J. Santos *et al.*, New J. Phys. **17**, 083051 (2015).

[20] U. Wagner, M. Tatarakis, A. Gopal, F. N. Beg, E. L. Clark, A. E. Dangor, R. G. Evans, M. G. Haines, S. P. D. Mangles, P. A. Norreys, M.-S. Wei, M. Zepf, and K. Krushelnick, Phys. Rev. E **70**, 026401 (2004).

[21] M. Tatarakis *et al.*, Phys. Plasmas **9**, 2244 (2002).

[22] M. Borghesi, A. J. MacKinnon, A. R. Bell, R. Gaillard, and O. Willi, Phys. Rev. Lett. **81**, 112 (1998).